Compact Dual-Wideband BPF Based on Quarter-Wavelength Open Stub Loaded Half-Wavelength Coupled-Line

Jin Xu

School of Electronics and Information,
Northwestern Polytechnical University, Xi'an, 710072, P.R. China
E-mail: xujin227@nwpu.edu.cn

Abstract **—** In this paper, a novel dual-wideband bandpass filter (BPF) is presented by using quarter-wavelength open stub loaded half-wavelength coupled-line. Equivalent voltage-current analysis method is applied to analyze this structure, which shows it has two tunable transmission zeros and dual-wideband frequency response. As an example, a dual-wideband BPF covering 1.228/1.57/6.8 GHz for GPS (Link 1 and Link 2) and RFID applications is designed, fabricated and measured. The fabricated filter has a compact size of $0.043\lambda_g \times 0.213\lambda_g$. The measured results show that the fabricated filter has the merits of low insertion loss, good return loss and high band-to-band isolation. The proposed dual-band BPF also has a very simple physical topology and quick design procedure.

Index Terms **—** Bandpass filter (BPF), coupled-line, dual-wideband, stub-loaded resonator.

I. INTRODUCTION

Modern dual-mode communication system requires a dual-band bandpass filter (BPF) to enhance the electrical performance of the radio frequency end. In recent years, many structures have been proposed to meet the above requirement. In [1], two sets of uniform-impedance half-wavelength resonators are used to design a dual-narrowband BPF for 1.8 GHz DCS and 2.4 GHz WLAN applications. A dual-passband BPF with multi-spurious suppression is realized by using asymmetrical stepped-impedance resonators in [2]. In [3], compact dual-band BPFs with controllable bandwidths are proposed by using stub loaded multiple-mode resonator. In [4], the quad-mode resonator is applied to design a compact and high-selectivity dual-mode dual-band BPF. Modified coupled-line is another effective structure to design dual-band BPF. It is widely known that coupled-line is a classical structure used in single-band BPF design, mainly due to its compact 1-D planar physical configuration and high passband selectivity. In [5,6], S. Lee and Y. Lee firstly introduce capacitive or inductive stubs in traditional coupled-line structure to achieve dual-band frequency response, and the transverse dimension of coupled-line-type BPF is decreased simultaneously. However, these two dual-band BPFs suffer from relatively large circuit size, complicated physical topology and design procedure. In the author's previous work [7,8], two stub loaded coupled-line dual-band BPFs have been proposed, and a good filter performance and compact circuit size has been achieved. Nevertheless, the insertion loss in [7] and out-of-band rejection in [8] need further improvements. In addition, the bandwidth in [7] cannot meet the requirement of modern dual high-data-rate communication system.

In this paper, a novel quarter-wavelength open stub loaded half-wavelength coupled-line is proposed, which has dual-band frequency performance. By using a half-wavelength transmission line to cascade the proposed two stub loaded coupled-line, a dual-wideband BPF with large dual-band central frequency ratio can be designed. As an example, a dual-wideband BPF for 1.228/1.57 GHz GPS and 6.8 GHz RFID applications is designed, fabricated and measured. Equivalent voltage-current analysis method is applied to analyze this dual-band BPF, and the corresponding design rules are given for the filter design.

II. THEORY ANALYSIS

A. ABCD parameters and S parameters

Figure 1 (a) gives the transmission line model of proposed dual-wideband BPF. It consists of two quarter-wavelength open stub loaded half-wavelength coupled-line and one half-wavelength transmission line. In order to analyze this structure, equivalent voltage and current analysis method is used, and the corresponding model is given in Fig. 1 (b). Thus, the *ABCD* parameters of proposed dual-wideband BPF can be given as follows:

Submitted On: June 17, 2014
Accepted On: June 4, 2015

$$\begin{bmatrix} A_F & B_F \\ C_F & D_F \end{bmatrix} = \begin{bmatrix} A_{ci} & B_{ci} \\ C_{ci} & D_{ci} \end{bmatrix} \begin{bmatrix} A_t & B_t \\ C_t & D_t \end{bmatrix} \begin{bmatrix} A_{co} & B_{co} \\ C_{co} & D_{co} \end{bmatrix}, \tag{1}$$

where

$$\begin{bmatrix} A_t & B_t \\ C_t & D_t \end{bmatrix} = \begin{bmatrix} \cos(2\theta) & jZ\sin(2\theta) \\ jY\sin(2\theta) & \cos(2\theta) \end{bmatrix} \quad Y = 1/Z.$$

If even-mode electrical length of coupled-line (θ_e) equaling to odd-mode electrical length of coupled-line (θ_o) are assumed, the following two equations can be obtained from the [9] as follows:

$$\begin{bmatrix} v_1 - v_2 \\ i_1 - i_2 \end{bmatrix} = \begin{bmatrix} \cos(2\theta) & jZ_{co}\sin(2\theta) \\ jY_{co}\sin(2\theta) & \cos(2\theta) \end{bmatrix} \begin{bmatrix} v_4 - v_3 \\ -(i_4 - i_3) \end{bmatrix}, \tag{2a}$$

$$\begin{bmatrix} v_1 + v_2 \\ i_1 + i_2 \end{bmatrix} = \begin{bmatrix} \cos(2\theta) & jZ_{ce}\sin(2\theta) \\ jY_{ce}\sin(2\theta) & \cos(2\theta) \end{bmatrix} \begin{bmatrix} v_4 + v_3 \\ -(i_4 + i_3) \end{bmatrix}, \tag{2b}$$

where

$$Z_{ce} = Z_c\sqrt{(1+k_c)/(1-k_c)} \quad Y_{ce} = 1/Z_{ce},$$
$$Z_{co} = Z_c\sqrt{(1-k_c)/(1+k_c)} \quad Y_{co} = 1/Z_{co}.$$

The coupled-line in Fig. 1 (b) has the boundary condition of $v_3 = -i_3 Z_L = j i_3 Z_s \cot\theta$ and $v_4 = 0$. After substituting these two conditions into the equations (2), the *ABCD* matrix of quarter-wavelength open stub loaded half-wavelength coupled-line can be derived as:

$$\begin{bmatrix} A_{ci} & B_{ci} \\ C_{ci} & D_{ci} \end{bmatrix} = \begin{bmatrix} \dfrac{u_1}{u_5} & -\dfrac{u_3}{u_7} + \dfrac{u_1 u_6}{u_5 u_7} \\ \dfrac{u_2}{u_5} & -\dfrac{u_4}{u_7} + \dfrac{u_2 u_6}{u_5 u_7} \end{bmatrix}, \tag{3a}$$

$$\begin{bmatrix} A_{co} & B_{co} \\ C_{co} & D_{co} \end{bmatrix} = \frac{1}{u_1 u_4 - u_2 u_3} \begin{bmatrix} u_4 u_5 - u_2 u_6 & -u_1 u_6 + u_3 u_5 \\ -u_2 u_7 & -u_1 u_7 \end{bmatrix}, \tag{3b}$$

where

$$u_1 = -j\left[(Z_{ce} + Z_{co})\sin(2\theta)\right]/2,$$
$$u_2 = -\cos(2\theta),$$
$$u_3 = j\left[(Z_{co} - Z_{ce})\sin(2\theta)\right]/2,$$
$$u_4 = \left[(Y_{co} - Y_{ce})Z_s\cot\theta\sin(2\theta)\right]/2,$$
$$u_5 = -j\left[(Z_{co} - Z_{ce})\sin(2\theta)\right]/2,$$
$$u_6 = j\left[2Z_s\cot\theta\cos(2\theta) - (Z_{ce} + Z_{co})\sin(2\theta)\right]/2,$$
$$u_7 = -\frac{2\cos(2\theta) + (Y_{ce} + Y_{co})Z_s\cot\theta\sin(2\theta)}{2}.$$

Since the proposed dual-wideband BPF is symmetrical, its *S*-parameters can be then given by:

$$S_{11} = S_{22} = \frac{A_F + B_F/Z_0 - C_F Z_0 - D_F}{A_F + B_F/Z_0 + C_F Z_0 + D_F}, \tag{4a}$$

$$S_{21} = S_{12} = \frac{2(A_F D_F - B_F C_F)}{A_F + B_F/Z_0 + C_F Z_0 + D_F}. \tag{4b}$$

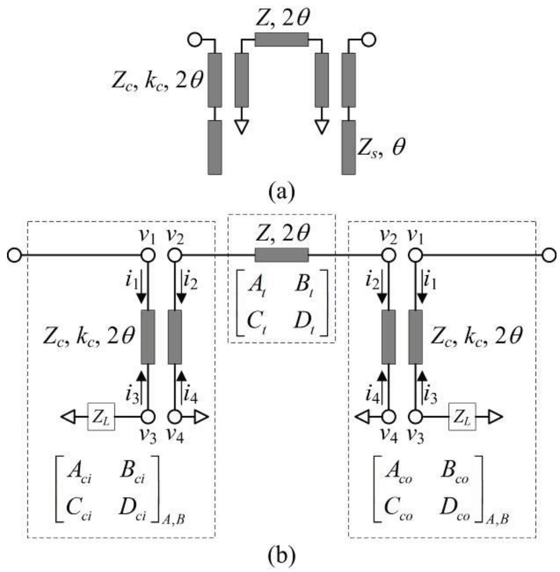

Fig. 1. (a) Transmission line model of proposed dual-wideband BPF, and (b) equivalent voltage and current analysis model.

B. Transmission zeros

The transmission zeros of proposed dual-wideband BPF is dependent on the quarter-wavelength open stub loaded half-wavelength coupled-line and independent on the half-wavelength transmission lines, so that the transmission zeros satisfy:

$$A_{ci,o} D_{ci,o} = B_{ci,o} C_{ci,o}. \tag{5}$$

After simplifying the equations (3), it will be derived that:

$$u_1 u_4 = u_2 u_3. \tag{6}$$

When $\theta = 0$, $\pi/2$ and π at the designing frequency f_0, respectively, it can be verified that the equation (6) is built. Thus, the proposed dual-wideband BPF has fixed transmission zeros at 0, f_0 and $2f_0$, respectively, within the frequency range $[0, 2f_0]$. Substituting u_1~u_6 into the equation (6), it can be gotten that:

$$\tan^2\theta = \left(Z_c\sqrt{1-k_c^2} + 4Z_s\right) \Big/ \left(Z_c\sqrt{1-k_c^2}\right). \tag{7}$$

The proposed dual-wideband BPF has a pair of tunable transmission zeros which are symmetrical along f_0. Its frequency locations are given as follows:

$$f_{z1} = \frac{2f_0}{\pi}\arctan\left(\sqrt{\frac{Z_c\sqrt{1-k_c^2} + 4Z_s}{Z_c\sqrt{1-k_c^2}}}\right), \tag{8a}$$

$$f_{z2} = \frac{2f_0}{\pi}\left(\pi - \arctan\left(\sqrt{\frac{Z_c\sqrt{1-k_c^2} + 4Z_s}{Z_c\sqrt{1-k_c^2}}}\right)\right). \tag{8b}$$

These two transmission zeros have the relationship of $0 < f_{z1} < f_0 < f_{z2} < 2f_0$, and repeat at every frequency range $[2nf_0, 2(n+1)f_0]$, where n is an integer.

C. Design rules

It can be verified that the proposed dual-wideband BPF has a symmetrical frequency response along the design frequency f_0. That is, two passbands of the proposed dual-wideband BPF has an equal value of absolute bandwidth BW. Under the initial designing parameters of Z = 140 Ω and k_c = 0.4, Fig. 2 plots the variation of f_{c2}/f_{c1} and BW/f_0 versus different values of $r_c = Z_c/Z$ and $r_s = Z_s/Z$, where f_{c1} and f_{c2} represents the central frequency of the first and second passband, respectively. It can be seen in Fig. 2 that f_{c2}/f_{c1} increases as r_c increases, but it decreases as r_s increases. It can be also seen in Fig. 2 that BW increases as r_s increases, and as r_c increases, BW increases firstly but then decreases. Figure 3 gives the variation of $|S_{21}|$ and $|S_{11}|$ versus different values of Z and k_c under fixed $r_c = r_s = 1.0$. It can be seen in Fig. 3 (a) that Z has minor effect on $|S_{21}|$ but it can be used to tune the $|S_{11}|$ slightly. It can be seen in Fig. 3 (b) that the BW of two passbands becomes wide as k_c increases.

In summary, in the dual-wideband design process, the designing parameters r_s and r_c can be tuned to achieve the desired frequency position of two passbands. The designing parameter k_c can be used to control the BW of two passbands and the designing parameter Z can be then tuned to acquire a good return loss. In addition, it should be noted that the BW of two passbands cannot be controlled individually due to its symmetrical frequency response.

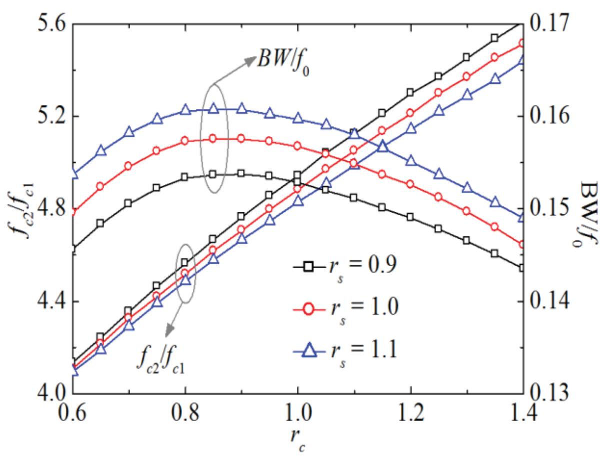

Fig. 2. Variation of f_{c2}/f_{c1} and BW/f_0 versus different values of r_c and r_s.

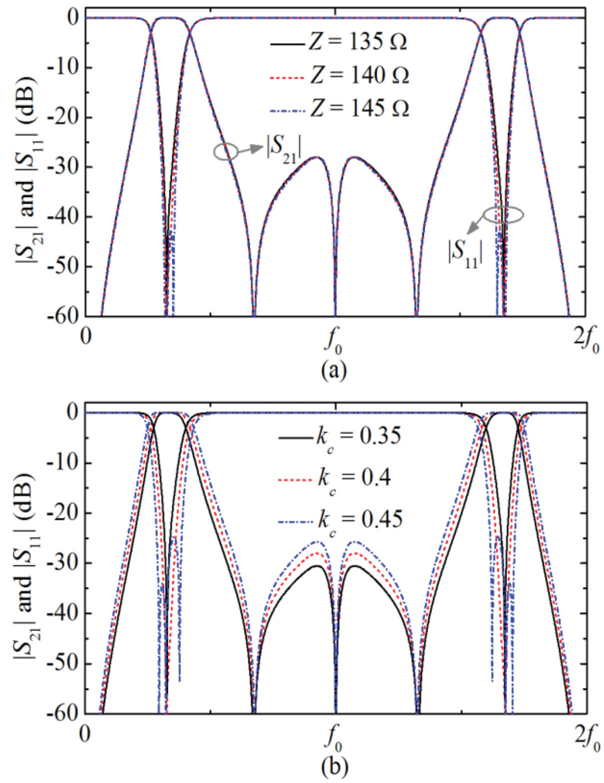

Fig. 3. Variation of $|S_{21}|$ and $|S_{11}|$ versus different values of: (a) Z (k_c = 0.4 fixed), and (b) k_c (Z = 140 Ω fixed).

III. SIMULATION AND MEASUREMENT

According to the above discussion, the initial designing parameters of dual-wideband BPF are pre-selected as Z_c = 147 Ω, k_c = 0.42, Z = 140 Ω and Z_s = 150 Ω, under which the first passband covers 1.228/1.575 GHz and the second passband covers 6.8 GHz. The dual-wideband BPF is designed on the substrate ARlon DiClad 880 (ε_{re} = 2.2, h = 0.508 mm, tanδ = 0.0009). Figure 4 (a) gives the layout of fabricated dual-wideband BPF. In Fig. 4 (a), the half-wavelength microstrip line and the loaded quarter-wavelength stubs are folded, so as to achieve size reduction. The whole structure is optimized by using the full wave EM simulator HFSS to consider the impact of bends, the grounded vias, the impedance discontinuities and the unequal even-/odd-mode phase velocities. The optimized physical dimensions are also labeled in Fig. 4 (a). Figure 4 (b) shows the photograph of fabricated dual-wideband BPF with the circuit size of $0.043\lambda_g \times 0.213\lambda_g$, where λ_g represents the guided wave-length of 50 Ω microstrip line at the central frequency of the first passband.

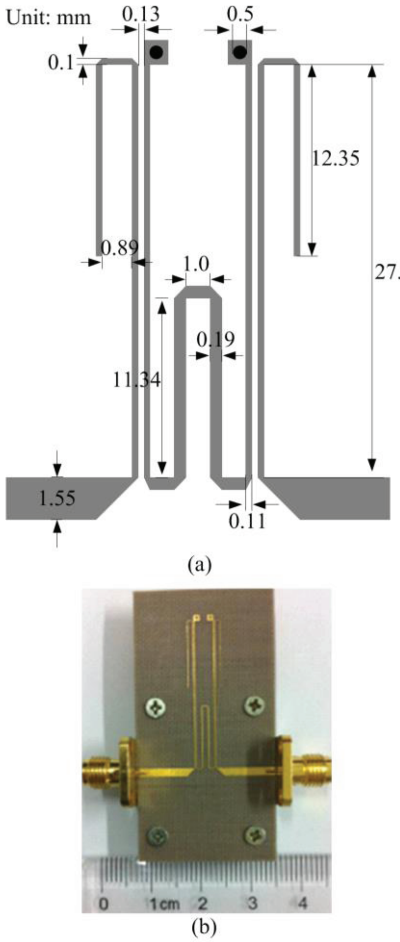

Fig. 4. (a) Layout, and (b) photograph of fabricated dual-wideband BPF.

The simulated and measured results of fabricated dual-band BPF are plotted in Fig. 5. Good agreement can be observed between the simulation and measurement. There are some discrepancies which are attributed to the fabrication error as well as SMA connectors. The measured central frequencies (CFs) and 3 dB FBW of two passbands are 1.54 GHz / 6.88 GHz and 60%/11.5%, respectively. The measured insertion losses (ILs) at 1.228 GHz, 1.575 GHz and 6.8 GHz are 0.4 dB, 0.4 dB and 0.9 dB, respectively. The return losses of two passbands are better than 26 dB and 15 dB, respectively. The band-to-band isolation is better than 20 dB from 2.5 GHz to 6.1 GHz.

Table 1 gives a performance comparison with some reported coupled-line-type dual-band BPF. In Table 1, CF, FBW and IL represents the central frequency, fractional bandwidth and insertion loss, respectively. After comparison, it obviously shows that the proposed dual-wideband BPF has the merits of low insertion loss, compact circuit size, wide passband, large dual-band central frequency ratio, simple physical topology and quick design procedure.

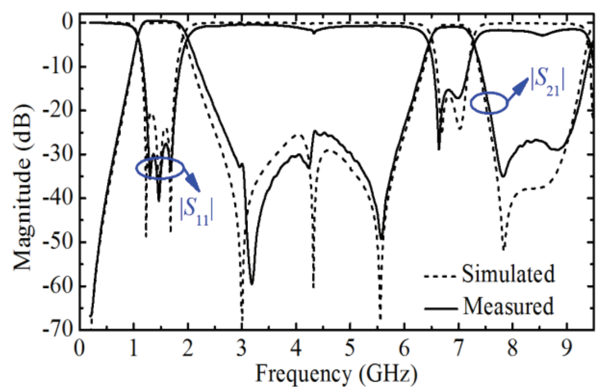

Fig. 5. Simulated and measured results of fabricated dual-wideband BPF.

Table 1: Performance comparison with some reported coupled-line-type dual-band BPFs

	CF (GHz)	3 dB FBW	IL at CF (dB)	Circuit Size (λ_g^2)
Ref. [5]	2.4, 5.2	8%, 3.69%	1.6, 2.5	0.189×0.733
Ref. [6] (Filter B)	2.0, 5.0	12%, 3%	1.0, 3.0	-
Ref. [7] (Filter A)	2.4, 5.8	5.8%, 2.1%	1.59, 2.59	0.312×0.304
Ref. [8] (Filter B)	2.48, 6.63	43.2%, 16.5%	0.33, 0.74	0.12×0.17
This Work	1.54, 6.88	60%, 11.5%	0.4, 0.9	0.043×0.213

IV. CONCLUSION

A dual-wideband BPF covering 1.228/1.57/6.8 GHz for GPS (Link 1 and Link 2) and RFID applications is presented by using proposed quarter-wavelength open stub loaded half-wavelength coupled-line. The fabricated dual-wideband BPF has a compact circuit area of $0.043\lambda_g \times 0.213\lambda_g$. Measured results also show its merits of low insertion loss, good return loss, sharp passband selectivity and good band-to-band isolation. The proposed filter has simple topology and design procedure. All these merits make it attractive in modern dual-wideband communication system.

ACKNOWLEDGMENT

This work was supported in part by the National Natural Science Foundation of China under Grant 61401358, and in part by the Fundamental Research Funds for Central Universities under Grant

3102014JCQ01058 and No. 30920140122005.

REFERENCES

[1] X.-Y. Zhang, J. Shi, J.-X. Chen, and Q. Xue, “Dual-band bandpass filter design using a novel feed scheme,” *IEEE Microw. Wireless Compon. Lett.*, vol. 19, no. 6, pp. 350-352, Jun. 2009.

[2] M. Jiang, L.-M. Chang, and A. Chin, “Design of dual-passband microstrip bandpass filters with multi-spurious suppression,” *IEEE Microw. Wireless Compon. Lett.*, vol. 20, no. 4, pp. 199-201, Apr. 2010.

[3] F. C. Chen, Q. X. Chu, Z. H. Li, and X. H. Wu, “Compact dual-band bandpass filter with controllable bandwidths using stub loaded multiple-mode resonator,” *IET Microw. Antennas Propag.*, vol. 6, no. 10, pp. 1172-1178, Nov. 2012.

[4] J. Xu, W. Wu, and C. Miao, “Compact and sharp skirts microstrip dual-mode dual-band bandpass filter using a single quadruple-mode resonator (QMR),” *IEEE Trans. on Microw. Theory Tech.*, vol. 61, no. 3, pp. 1104-1113, Mar. 2013.

[5] S. Lee and Y. Lee, “A planar dual-band filter based on reduced-length parallel coupled lines,” *IEEE Microw. Wireless Compon. Lett.*, vol. 20, no. 1, pp. 16-18, Jan. 2010.

[6] S. Lee and Y. Lee, “A uniform coupled-line dual-band filter with different bandwidths,” *IEEE Microw. Wireless Compon. Lett.*, vol. 20, no. 10, pp. 545-547, Oct. 2010.

[7] J. Xu, C. Miao, and W. Wu, “A compact and high isolation dual-mode dual-band bandpass filter with tunable transmission zeros,” *J. of Electromagn. Waves and Appl.*, vol. 26, no. 17-18, pp. 2390-2397, Dec. 2012.

[8] J. Xu and W. Wu, “Compact microstrip dual-mode dual-band bandpass filters using stubs loaded coupled line,” *Progress In Electromagnetics Research C*, vol. 41, pp. 137-150, 2013.

[9] I. Z. George and A. K. Johnson, “Coupled transmission line networks in an inhomogeneous dielectric medium,” *IEEE Trans. on Microw. Theory Tech.*, vol. 17, no. 10, pp. 753-759, Oct. 1969.

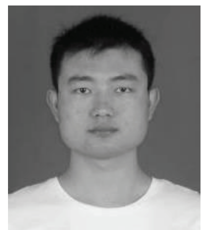

Jin Xu was born in AnHui Province, P.R. China, in 1987. He received the B.Eng. degree in Information Countermeasure Technology and the Ph.D. degree in Information and Communication Engineering from Nanjing University of Science and Technology (NUST), Nanjing, China, in 2009 and 2013, respectively. He is currently an Associate Professor with the School of Electronics and Information, Northwestern Polytechnical University, Xi’an, China. His research interests include UWB technology, MCM technology, microwave passive/active components, microwave and millimeter-wave MMICs developed on SiGe, phased array radar and wireless communication system.

From February 2011 to September 2011, he was an attached Ph.D. student in the Institute of Microelectronics, Singapore. From October 2011 to September 2012, he joined MicroArray Technologies Corporation Limited, Chengdu, P.R. China, where he was an IC R&D Engineer. Since 2011, he has served as a Reviewer for some journals including IEEE Microwave Wireless Component Letters, International Journal of Electronics, PIER and JEMWA.